

Research paper

# Development and characterization of PLGA nanospheres and nanocapsules containing xanthone and 3-methoxyxanthone

Maribel Teixeira<sup>a,b</sup>, Maria J. Alonso<sup>c</sup>, Madalena M.M. Pinto<sup>a</sup>, Carlos M. Barbosa<sup>d,e,\*</sup>

<sup>a</sup>Centro de Estudos de Química Orgânica, Fitoquímica e Farmacologia da Universidade do Porto-Faculdade de Farmácia do Porto, Porto, Portugal

<sup>b</sup>Instituto Superior de Ciências da Saúde-Norte, Gandra PRD, Portugal

<sup>c</sup>Laboratório de Farmácia Galénica, Facultad de Farmácia, Santiago de Compostela, Spain

<sup>d</sup>CTMUP/Faculdade de Farmácia do Porto, Porto, Portugal

<sup>e</sup>CETMED-Centro Tecnológico do Medicamento, Porto, Portugal

Received 23 June 2004; accepted in revised form 3 September 2004

Available online 30 October 2004

## Abstract

The aim of the present work was to develop and characterize two different nanosystems, nanospheres and nanocapsules, containing either xanthone (XAN) or 3-methoxyxanthone (3-MeOXAN), with the final goal of improving the delivery of these poorly water-soluble compounds. The xanthenes-loaded nanospheres (nanomatrix systems) and nanocapsules (nanoreservoir systems), made of poly(DL-lactide-co-glycolide) (PLGA), were prepared by the solvent displacement technique. The following characteristics of nanoparticle formulations were determined: particle size and morphology, zeta potential, incorporation efficiency, thermal behaviour, in vitro release profiles and physical stability at 4 °C. The nanospheres had a mean diameter <170 nm, a narrow size distribution (polydispersity index <0.1), and a negative surface charge (zeta potential <−36 mV). Their incorporation efficiencies were 33% for XAN and 42% for 3-MeOXAN. The presence of the xanthenes did not affect the nanospheres size and zeta potential. DSC studies indicated that XAN and 3-MeOXAN were dispersed at a molecular level within the polymeric nanomatrix. Nanocapsules were also nanometric (mean size <300 nm) and exhibited a negative charge (zeta potential <−36 mV). Their incorporation efficiency values (>77%) were higher than those corresponding to nanospheres for both xanthenes. The release of 3-MeOXAN from nanocapsules was similar to that observed for the correspondent nanoemulsion, indicating that drug release is mainly governed by its partition between the oil core and the external aqueous medium. In contrast, the release of XAN from nanocapsules was significantly slower than from the nanoemulsion, a behaviour that suggests an interaction of the drug with the polymer. Nanocapsule formulations exhibited good physical stability at 4 °C during a 4-month period for XAN and during a 3-month period for 3-MeOXAN.

© 2004 Elsevier B.V. All rights reserved.

**Keywords:** Xanthone; 3-Methoxyxanthone; Nanoparticles; Nanospheres; Nanocapsules; PLGA

## 1. Introduction

Xanthenes are natural, semisynthetic and totally synthetic heterocyclic compounds with the dibenzo- $\gamma$ -pyrone framework. Xanthone molecules having a variety of substituents on the different carbons of the nucleus constitute a group of compounds with a broad spectrum of

biological activities [1,2]. Among others, anti-inflammatory [3], hepatoprotective [4], immunomodulatory [5–7], modulatory activity of PKC isoforms [8,9] and antitumor activities of the growth of human cancer cell lines [7].

The poor aqueous solubility of xanthone (XAN) and of many of its derivatives such as 3-methoxyxanthone (3-MeOXAN) (Fig. 1) is a major drawback not only for their use in the therapy but even for the in vitro assessment of their biological activity. One approach to overcome the difficulty of administration of poorly water-soluble compounds is their incorporation in polymeric nanocarriers [10–12]. Depending on the processing conditions, either

\* Corresponding author. CTMUP/Faculdade de Farmácia do Porto, R. Aníbal Cunha, 164, 4050-047 Porto, Portugal. Tel.: +351 22 207 8900; fax: +351 22 200 3977.

E-mail address: [mauricio.barbosa@anf.pt](mailto:mauricio.barbosa@anf.pt) (C.M. Barbosa).

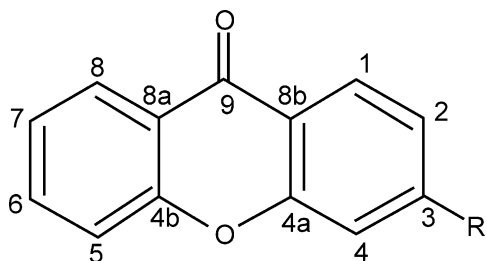


Fig. 1. Chemical structure of xanthenes: XAN (R=H), 3-MeOXAN (R=OCH<sub>3</sub>).

nanospheres or nanocapsules can be obtained [13]. Nanospheres are matrix-type systems composed of an entanglement of oligomer or polymer units, while nanocapsules are reservoir-type systems, consisting of an oily core surrounded by a polymer wall. Besides their ability to improve the delivery of water-insoluble drugs, nanoparticles have been reported to control drug release [10], to reduce drug-associated adverse effects [14], to protect the compounds from inactivation before reaching their site of action [15], to increase the intracellular penetration [16] and enhance the pharmacological activity [12].

Based on these considerations, the aim of the present work was to develop new formulations of XAN and 3-MeOXAN consisting of PLGA nanospheres and nanocapsules with the final goal of improving the biological activities of these compounds. The evaluation of the activity of these molecules, such as the inhibitory effect on nitric oxide (NO) production from macrophages and the inhibitory activity on different human cancer cell lines growth, represents a major interest of our research group.

PLGA was selected for the preparation of the nanocarriers because of its adequate biocompatibility and biodegradability [17]. Both systems, nanospheres and nanocapsules were prepared according to the solvent displacement technique described by Fessi et al. [18,19]. This is a simple method that is particularly useful for the encapsulation of lipophilic substances [13,20,21]. Formulations were characterized with regard to their particle size distribution, zeta potential, drug incorporation efficiency and thermal behaviour. In vitro drug release and stability studies were also performed for the most promising formulations.

## 2. Materials and methods

### 2.1. Materials

Xanthone (XAN), PLGA (50:50) MW 50 000–75 000, Pluronic F-68, phosphate buffered saline tablets and soybean lecithin (40% purity by thin-layer chromatography) were purchased from Sigma-Aldrich Química (Sintra, Portugal). Threalose dihydrate was purchased from Fluka (Sintra, Portugal). 3-Methoxyxanthone (3-MeOXAN) was synthesised in our laboratory according to Fernandes et al.

[22]. Myritol 318 (caprylic/capric acid triglyceride) was kindly supplied by Henkel (Lisboa, Portugal). HPLC-grade methanol and acetonitrile were obtained from Merck (Lisboa, Portugal). Water was purified by reverse osmosis Milli-Q system (Millipore<sup>®</sup>, Lisboa, Portugal). Other chemicals were of analytical grade.

### 2.2. Preparation of nanospheres

Nanospheres containing XAN or 3-MeOXAN were prepared by the solvent displacement technique described by Fessi et al. [18]. Briefly, an organic solution of PLGA (63 mg) and different amounts of XAN or 3-MeOXAN in acetone (10 mL) was poured, under moderate magnetic stirring, into 10 mL of an aqueous solution of Pluronic<sup>®</sup> F-68 0.25% (w/v). Following 5 min of stirring, the volume of nanosphere dispersion was concentrated to 10 mL under reduced pressure. Separation of non-encapsulated compounds was performed by centrifugation at 2000×g for 30 min. (Heraeus Sepatec centrifuge, Porto, Portugal) after solubilization of a certain amount of threalose dihydrate for achieving a 5% (w/v) concentration. The supernatant was discarded and the pellet containing the nanospheres was redispersed in water to complete the initial volume of nanosphere dispersion submitted to centrifugation. Empty nanospheres were prepared according to the same procedure but omitting the xanthenes in the organic phase.

### 2.3. Physicochemical characterization of nanospheres

#### 2.3.1. Particle size and zeta potential

Particle size analysis of nanospheres was performed by photon correlation spectroscopy (PCS). This technique yields the mean particle diameter and the polydispersity index (PI), which is a dimensionless measure of the broadness of the particle size distribution. Zeta potential was evaluated by laser Doppler anemometry (LDA). In both determinations, samples were analysed following appropriate dilution with filtered (0.22 μm) ultrapure water, using a Zetasizer 3000 (Malvern Instruments, Malvern, UK). Values reported are the mean ± SD of at least three different batches of each nanosphere formulation.

#### 2.3.2. Quantification of XAN and 3-MeOXAN content in nanospheres

The content of XAN and 3-MeOXAN of the nanospheres was determined by UV (Schimadzu UV 1603 spectrophotometer, Shimadzu Co., Kyoto, Japan) at 237 nm, by a modification of a previously validated method [23], following the dissolution of the nanospheres in acetonitrile. Previous studies demonstrated no absorbance interference from empty nanospheres under the same conditions.

Incorporation efficiency was calculated as follows:

$$\text{I.E.(\%)} = A/B \times 100$$

where  $A$  is the drug concentration ( $\mu\text{g/mL}$ ) in the nanosphere dispersion and  $B$  is the theoretical drug concentration ( $\mu\text{g/mL}$ ).

### 2.3.3. Differential scanning calorimetry (DSC)

DSC was performed in order to characterize the physical state of XAN and 3-MeOXAN in nanospheres. Thermograms were obtained using a Shimadzu DSC-50 (Shimadzu Co., Kyoto, Japan). The adopted scanning temperature range was from 25 to 300 °C at a heating rate of 10 °C/min.

### 2.3.4. Morphological studies

Morphological examination of nanospheres was performed by transmission electron microscopy (TEM) (Zeiss microscope M-10C, New York, USA) following negative staining with uranyl acetate solution (1%, w/v) or phosphotungstic acid solution (2%, w/v).

## 2.4. Preparation of nanocapsules

XAN and 3-MeOXAN-containing PLGA nanocapsules were prepared by the interfacial polymer deposition technique described by Fessi et al. [19]. Briefly, about 50 mg of polymer and 100 mg of soybean lecithin were dissolved in 10 mL of acetone. Different amounts of XAN or 3-MeOXAN were dissolved in 0.5–0.6 mL of *Myritol*<sup>®</sup> 318 and the solution obtained was added to the previously prepared acetonic solution. The final solution was poured into 20 mL of an aqueous solution of *Pluronic*<sup>®</sup> F-68 0.5% (w/v) under moderate stirring, leading to the formation of the nanocapsules. Then, acetone was removed under vacuum and the colloidal dispersion of nanocapsules was concentrated to 5–10 mL by evaporation under reduced pressure. The amount of non-encapsulated xanthenes (either XAN or 3-MeOXAN) was separated by ultrafiltration/centrifugation technique [19] using centrifugal filter devices (Centricon YM-50, Millipore<sup>®</sup>, Lisboa, Portugal) at 4000× $g$  for 2 h (Beckman UL-80 ultracentrifuge, Albertville, USA). Empty nanocapsules were prepared according to the same procedure but omitting the xanthenes in the organic phase.

XAN and 3-MeOXAN nanoemulsions were prepared as nanocapsules, omitting the polymer in the organic phase.

## 2.5. Physicochemical characterization of nanocapsules

### 2.5.1. Particle size and zeta potential

Particle size analysis of nanocapsules was performed by photon correlation spectroscopy (PCS). This technique yields the mean particle diameter and the polydispersity index (PI), which is a dimensionless measure of the broadness of the particle size distribution. Zeta potential was evaluated by laser Doppler anemometry (LDA). In both determinations, samples were analysed following

appropriate dilution with filtered (0.22  $\mu\text{m}$ ) ultrapure water, using a Zetasizer 5000 (Malvern Instruments, Malvern, UK). Values reported are the mean  $\pm$  SD of at least three different batches of each nanocapsule formulation.

### 2.5.2. Quantification of XAN and 3-MeOXAN content in nanocapsules

The content of XAN and 3-MeOXAN of the nanocapsules was determined by a previously validated HPLC method [24], following the dissolution of an aliquot of the nanocapsule dispersion in acetonitrile.

Incorporation efficiency was calculated as described for nanospheres (Section 2.3.2).

### 2.5.3. In vitro release studies of XAN and 3-MeOXAN from nanocapsules

In vitro release studies of XAN and 3-MeOXAN from the nanocapsules were carried out at 37 °C, by the bulk equilibrium reverse dialysis bag technique, as previously described by Levy and Benita [25]. Briefly, for each xanthonic compound, a volume of a nanocapsule dispersion—corresponding to 20% of the maximum aqueous solubility of each compound in phosphate buffered saline solution 0.1 M, pH7.4 (PBS) at 37 °C—or an aqueous solution, was placed directly into 200 mL of PBS, where numerous dialysis sacs (cellulose membrane Mw cut-off 12 000 D, Sigma-Adrich Química, Sintra, Portugal) containing 1 mL of PBS, had been previously immersed. The dialysis sacs were equilibrated with PBS prior to the experiments. At given time intervals, a dialysis bag was withdrawn from the stirred release medium and the XAN or 3-MeOXAN content was directly assayed by a modification of a previously validated HPLC method [24], setting the detection wavelength at 240 nm. XAN or 3-MeOXAN stock solutions in acetonitrile were diluted with PBS to obtain calibration solutions over the range of 0.1–1.4  $\mu\text{g/mL}$ . Values reported are the mean  $\pm$  SD of the values corresponding to three different batches of each formulation of nanocapsules.

### 2.5.4. Physical stability

The effect of storage time on the particle size and zeta potential of XAN and 3-MeOXAN-containing nanocapsules formulations was assessed. Nanocapsules aqueous dispersions were stored in sealed glass bottles at 4 °C and protected from light, during a 4-month period.

### 2.5.5. Morphological studies

The morphology of nanocapsules was assessed by TEM using a Zeiss EM-10C microscope (New York, USA), following negative staining with phosphotungstic acid solution (2%, w/v).

Table 1  
Encapsulation parameters of XAN and 3-MeOXAN in PLGA nanospheres

Theoretical concentration ( $\mu\text{g/mL}$ )	XAN nanospheres		3-MeOXAN nanospheres	
	Final concentration ( $\mu\text{g/mL}$ )	Encapsulation efficiency (%)	Final concentration ( $\mu\text{g/mL}$ )	Encapsulation efficiency (%)
50	$13.0 \pm 1.1$	$26.1 \pm 2.1$	$19.0 \pm 0.6$	$38.1 \pm 1.1$
60	$20.0 \pm 2.4$	$33.0 \pm 4.1$	$24.9 \pm 4.6$	$41.5 \pm 7.6$
70	Crystals of XAN	ND	Crystals of 3-MeOXAN	ND
80	Crystals of XAN	ND	Crystals of 3-MeOXAN	ND

Values express the mean results  $\pm$  SD values of three different batches. ND, not determined.

Table 2  
Mean diameter, polydispersity index (PI) and zeta potential ( $\zeta$ ) of PLGA empty and loaded nanospheres

	Empty nanospheres	XAN nanospheres <sup>a</sup>	3-MeOXAN nanospheres <sup>b</sup>
Diameter (nm)	$154 \pm 6$	$164 \pm 8$	$164 \pm 9$
PI	$0.06 \pm 0.03$	$0.06 \pm 0.03$	$0.06 \pm 0.01$
$\zeta$ (mV)	$-36.2 \pm 5.2$	$-38.9 \pm 1.3$	$-36.0 \pm 3.0$

Values express the mean results  $\pm$  SD values of three different batches.

<sup>a</sup> XAN nanosphere with theoretical concentration of  $60 \mu\text{g/mL}$ .

<sup>b</sup> 3-MeOXAN nanospheres with theoretical concentration of  $60 \mu\text{g/mL}$ .

### 3. Results and discussion

#### 3.1. Characteristics of XAN and 3-MeOXAN-loaded nanospheres

The loading capacity of the nanospheres was assessed using fixed amounts of polymer and surfactant and variable quantities of XAN or 3-MeOXAN. According to the results shown in Table 1, maximum incorporation efficiencies were achieved either for XAN ( $33.0 \pm 4.1\%$ ) or for 3-MeOXAN ( $41.5 \pm 7.6\%$ ) corresponding to a theoretical concentration of  $60 \mu\text{g/mL}$ . For concentrations above  $70 \mu\text{g/mL}$  both xanthenes precipitated in the form of crystals, indicating that the maximum loading capacity of the carrier was reached. Thus, for the theoretical concentration of  $60 \mu\text{g/mL}$ , the final concentrations of encapsulated

compounds were only of  $20 \mu\text{g/mL}$  for XAN and  $25 \mu\text{g/mL}$  for 3-MeOXAN. According to Barichello et al. [26] when the drug has a low affinity for the polymer, it tends to diffuse from the organic phase to the external aqueous medium during the nanosphere formation process, leading to low drug loading capacities. The relatively low association efficiency observed in the present study for XAN and 3-MeOXAN, suggests that these compounds have low affinity for the polymer. In fact, for the theoretical concentration of  $60 \mu\text{g/mL}$ , the final concentrations achieved for encapsulated compounds were only of  $20$  and  $25 \mu\text{g/mL}$  for XAN and 3-MeOXAN, respectively. Nevertheless, the nanosphere aqueous dispersions developed show higher concentrations for both xanthenes than the respective aqueous solutions. Indeed the water-solubility of both xanthenes is about  $5\text{--}6 \mu\text{g/mL}$  at  $25^\circ\text{C}$  (data not shown).

Particle size results (Table 2) of prepared empty XAN and 3-MeOXAN nanospheres showed that all samples were in the nanometric range (mean diameter  $<170$  nm) and exhibited a narrow size distribution ( $\text{PI} < 0.1$ ). These results were confirmed by TEM analysis. In fact, TEM microphotographs of XAN- and 3-MeOXAN-loaded nanospheres (Fig. 2) show their spherical shape as well as their homogeneous size distribution. Similar results have been previously reported for PLGA nanoparticles containing various drugs [26].

Zeta potential results (Table 2) showed that both empty and drug-loaded nanosphere formulations exhibited a negative charge with values ranging from  $-38.9$  to  $-36.0$  mV, typically observed for these types of systems [27]. The surface charge of colloidal particles can arise by a number of means, e.g. ionisation of chemical groups on the surface or adsorption of ions [28]. It has been previously reported [29,30] that the negative charge of PLGA nanoparticles is due to the ionisation of carboxylic-end groups of polymer on the surface. However, carboxylic end groups of the PLGA used in this study were esterified with lauryl groups and hence were not susceptible to ionisation. Thus, the negative charge of prepared nanoparticles can be attributed to the adsorption of anions on the colloidal surface. The presence of both xanthenes did not

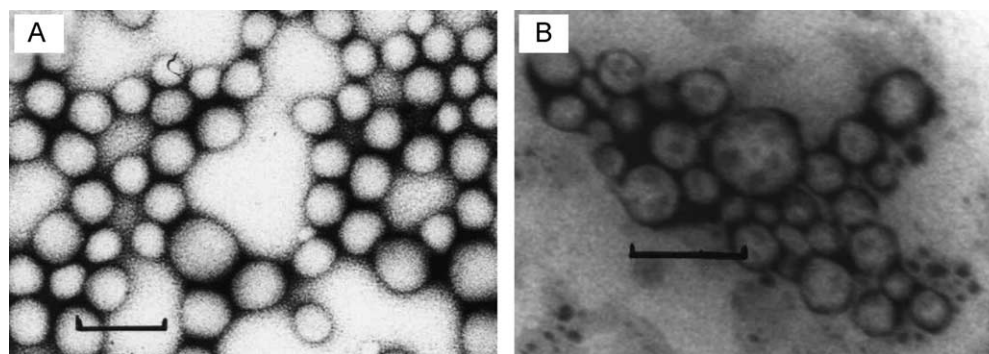


Fig. 2. Transmission electron microphotographs of PLGA nanospheres containing: (A) XAN or (B) 3-MeOXAN. Scale bar = 150 nm.

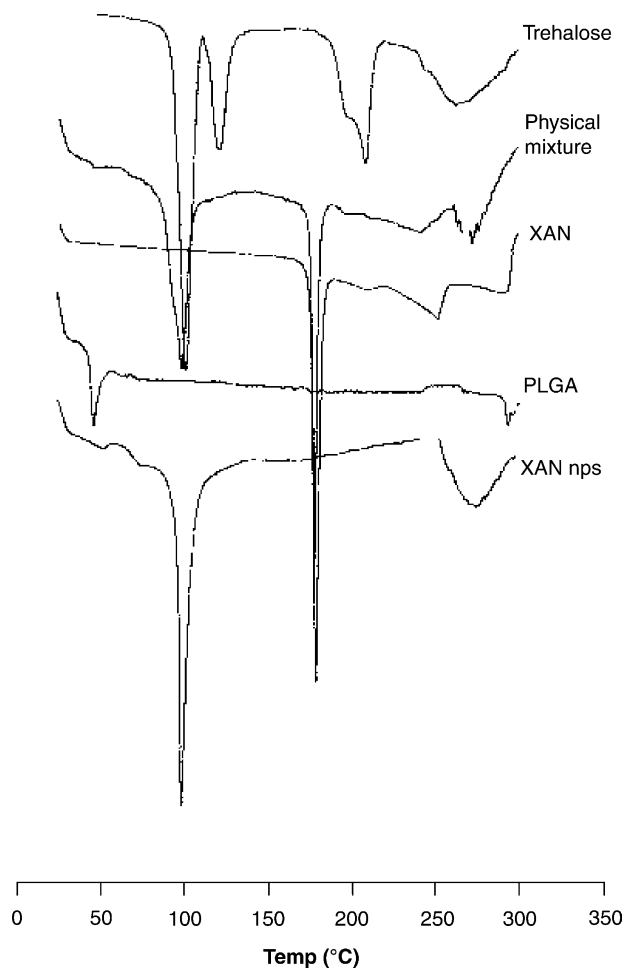


Fig. 3. DSC thermograms of trehalose, physical mixture of XAN and empty PLGA nanospheres (1:1), XAN, PLGA and XAN-loaded nanospheres (XAN nps).

significantly affect either the mean diameter or the zeta potential of nanospheres ( $P > 0.05$ ).

Fig. 3 shows the DSC thermograms corresponding to the following samples: PLGA; XAN; trehalose; a physical mixture of XAN and empty nanospheres (1:1) and XAN-loaded nanospheres. The PLGA thermogram displays an endotherm at 46 °C, corresponding to the polymer glass transition temperature ( $T_g$ ) and the trehalose thermogram shows an endotherm attributed to the dehydration of the compound, which occurred at 98 °C. The thermogram of XAN displays a thermal event at 178 °C, attributed to its melting point. Physical mixture of XAN and empty nanospheres (1:1) exhibits endotherms corresponding to the  $T_g$  of PLGA, to the dehydration of trehalose as well as to the melting point of XAN. For XAN-loaded nanospheres a thermal event at 98 °C, attributed to trehalose crystal dehydration was observed and it was not possible to clearly identify whether the polymer  $T_g$  has suffered any significant change. Furthermore, since no XAN melting endotherm was observed we might conclude that there are no crystalline XAN domains in nanospheres.

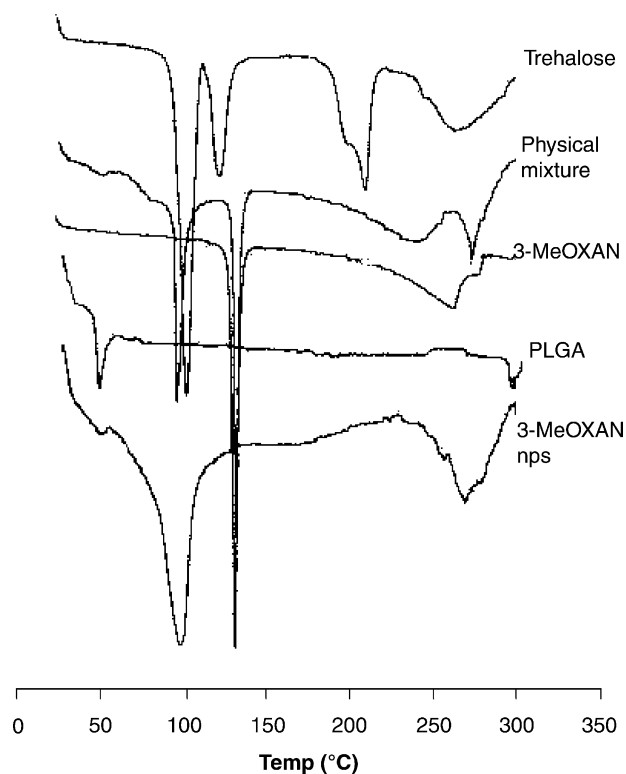


Fig. 4. DSC thermograms of trehalose, physical mixture of 3-MeOXAN and empty PLGA nanospheres (1:1), 3-MeOXAN, PLGA and 3-MeOXAN-loaded nanospheres (3-MeOXAN nps).

Fig. 4 shows DSC thermograms corresponding to the following samples: PLGA; 3-MeOXAN; trehalose; physical mixture of 3-MeOXAN and empty nanospheres (1:1) and 3-MeOXAN-loaded nanospheres. The thermogram of 3-MeOXAN shows a thermal event at 131 °C corresponding to its melting point. The physical mixture of 3-MeOXAN and empty PLGA nanospheres exhibits endotherms corresponding to the  $T_g$  of PLGA, to the dehydration of trehalose as well as to the melting point of 3-MeOXAN. The thermogram of 3-MeOXAN-loaded nanospheres shows an endotherm corresponding to trehalose dehydration (at 98 °C) and a mild thermal event at approximately at 46 °C, which may correspond to the  $T_g$  of the polymer. However, the melting endotherm of 3-MeOXAN was not detected. Consequently, these data suggest that both XAN and 3-MeOXAN form a molecular dispersion in the polymer matrix of nanospheres.

### 3.2. Characteristics of XAN and 3-MeOXAN-loaded nanocapsules

Two strategies were adopted in order to prepare stable nanocapsule dispersions containing a high concentration of both xanthenes. One of them was based on increasing the concentration of xanthenes added to the oily core of the nanocapsules until the precipitation of the excess — non-encapsulated — occurred and could be observed. For this

Table 3  
Encapsulation parameters of XAN and 3-MeOXAN in PLGA nanocapsules

XAN nanocapsules				3-MeOXAN nanocapsules			
Theoretical concentration ( $\mu\text{g/mL}$ )	XAN/Myritol 318% (w/v)	Final concentration ( $\mu\text{g/mL}$ )	Encapsulation efficiency (%)	Theoretical concentration ( $\mu\text{g/mL}$ )	3-MeOXAN/Myritol 318% (w/v)	Final concentration ( $\mu\text{g/mL}$ )	Encapsulation efficiency (%)
200	0.4	178 $\pm$ 21	89 $\pm$ 11	1000	2.0	887 $\pm$ 51	89 $\pm$ 5
400	0.8	342 $\pm$ 18	85 $\pm$ 5	1200	2.4	918 $\pm$ 9	77 $\pm$ 1
600	1.2	529 $\pm$ 57	88 $\pm$ 9	1400	2.8	1162 $\pm$ 80	83 $\pm$ 6
700	1.4	Crystals of XAN	ND	1600	3.2	Crystals of 3-MeOXAN	ND
800	1.6	Crystals of XAN	ND				

Values express the mean results  $\pm$  SD values of three different batches. ND, not determined.

purpose, different batches of XAN or 3-MeOXAN nanocapsules were prepared using fixed amounts of polymer (PLGA), surfactants (*Pluronic F-68* and soybean lecithin) and 0.5 mL of oil and increasing theoretical concentrations of xanthenes in the final suspension ranging from 200 to 800  $\mu\text{g/mL}$  for XAN and from 1000 to 1600  $\mu\text{g/mL}$  for 3-MeOXAN. The resulting incorporation efficiency values were close to 90% for XAN formulations with theoretical concentrations ranging from 200 to 600  $\mu\text{g/mL}$  (Table 3). For higher concentrations, XAN crystals could be observed, indicating that the maximum loading capacity of the nanocapsules had been reached. For the 3-MeOXAN-loaded nanocapsules, the incorporation efficiency values were close to 80% for theoretical concentrations ranging from 1000 to 1400  $\mu\text{g/mL}$ . As in the previous case, for higher concentrations, 3-MeOXAN crystals could be detected. Hence, maximum concentrations of xanthenes encapsulated into the nanocapsules were attained for theoretical concentrations of 600  $\mu\text{g/mL}$  for XAN (corresponding to a concentration of 1.2%, w/v, in *Myritol 318*) and 1400  $\mu\text{g/mL}$  for 3-MeOXAN (corresponding to a concentration of 2.8%, w/v, in *Myritol 318*). According to different authors [31–33], the percentage of drug encapsulated in the nanocapsules is correlated to the drug solubility in the oil core. In the present case, the incorporation efficiency values of both xanthenes were relatively close. However, the final concentration of the nanoencapsulated 3-MeOXAN (1162  $\mu\text{g/mL}$ ) was higher than that of XAN (529  $\mu\text{g/mL}$ ). An explanation for these results may be the higher solubility of 3-MeOXAN in *Myritol 318* than XAN.

The second strategy adopted in order to increase the concentration of the nanoencapsulated xanthenes in the nanocapsules suspension was based on increasing the volume of *Myritol 318* and on concentrating the final dispersion to 5 mL instead of 10 mL. When using this strategy, one must be aware of the fact that, as observed by Guterres et al. [31] for PLA nanocapsules containing diclofenac, the increase of the oil volume can eventually reduce the stability of nanocapsules. More specifically, these authors found that the use of a volume of oil (benzylbenzoate) higher than 0.75 mL (corresponding to a concentration

of 5%, v/v), led to the formation of unstable nanocapsules with the appearance of a precipitate and free oil. A common method used to study the stability of nanocapsules is the ultracentrifugation [34,35]. When nanocapsule dispersions prepared with an oil core with a density  $< 1$ , such as *Myritol 318*, are submitted to centrifugation four possible phases can be detected. One is constituted by a small pellet attributed to the formation of nanospheres due to the inadequate polymer deposition at the interfacial level. An additional phase may be found containing surfactants and non-encapsulated compounds. A floating cream layer corresponding to stable nanocapsules constitutes the third one. Finally, an oily phase may appear at the surface of the preparation due to oil drops that coalesced when surfactants could not stabilize the preparation.

In the present work, to study the stability of nanocapsules prepared with high oil volumes ( $> 0.5$  mL), several formulations of empty nanocapsules were obtained using fixed amounts of polymer and surfactants and different volumes of *Myritol 318* (0.5, 0.6, 0.7 and 0.8 mL) and submitted to centrifugation (25 000  $\times g$ , for 30 min). The formulations containing 0.5 and 0.6 mL of *Myritol 318* showed a small pellet at the bottom of the flask, attributed to nanospheres and a cream layer at the surface corresponding to nanocapsules. No free oil could be detected in these formulations indicating that the oil was completely coated by the polymer. The formulations including 0.7 and 0.8 mL of *Myritol 318* showed a free oil layer at the surface of the dispersions upon centrifugation indicating a poor stability.

Table 4  
Mean diameter, polydispersity index (PI) and zeta potential ( $\zeta$ ) of empty and loaded PLGA nanocapsules

	Empty nanocapsules	XAN nanocapsules <sup>a</sup>	3-MeOXAN nanocapsules <sup>b</sup>
Diameter (nm)	274 $\pm$ 3	278 $\pm$ 15	280 $\pm$ 19
PI	0.455 $\pm$ 0.130	0.412 $\pm$ 0.051	0.376 $\pm$ 0.104
$\zeta$ (mV)	-40.9 $\pm$ 5.9	-39.1 $\pm$ 0.7	-39.5 $\pm$ 4.7

Values express the mean results  $\pm$  SD values of three different batches.

<sup>a</sup> XAN nanocapsules with theoretical concentration of 600  $\mu\text{g/mL}$ .

<sup>b</sup> 3-MeOXAN nanocapsules with theoretical concentration of 1400  $\mu\text{g/mL}$ .

Table 5

Mean diameter, polydispersity index (PI), zeta potential ( $\zeta$ ) and incorporation parameters of various nanocapsule formulations: empty nanocapsules (0.6 mL *Myritol 318* and without xanthenes), XAN-loaded nanocapsules (0.6 mL *Myritol 318*, XAN theoretical concentration of 1440  $\mu\text{g/mL}$ ) and 3-MeOXAN-loaded nanocapsules (0.6 mL *Myritol 318*, 3-MeOXAN theoretical concentration of 3360  $\mu\text{g/mL}$ )

Sample	Theoretical concentration ( $\mu\text{g/mL}$ )	Final concentration ( $\mu\text{g/mL}$ ) [n]	Encapsulation efficiency (%)	Diameter (nm) [n]	PI	$\zeta$ (mV) [n]
Empty nanocapsules	–	–	–	261 $\pm$ 17 [5]	0.48 $\pm$ 0.06	–36.3 $\pm$ 4.3 [5]
XAN nanocapsules	1440	1173 $\pm$ 100 [7]	82 $\pm$ 7	273 $\pm$ 18 [5]	0.48 $\pm$ 0.05	–36.4 $\pm$ 9.3 [5]
3-MeOXAN nanocapsules	3360	2780 $\pm$ 238 [7]	83 $\pm$ 7	271 $\pm$ 16 [5]	0.43 $\pm$ 0.03	–41.8 $\pm$ 5.4 [5]

Thus, our results suggest that 0.6 mL is the limiting volume of *Myritol 318* that allows the preparation of stable nanocapsule formulations. As a consequence, the new formulations of XAN and 3-MeOXAN-containing nanocapsules were prepared using 0.6 mL of *Myritol 318*, while maintaining the concentration of each compound in the oil volume (1.2%, w/v, for XAN and 2.8%, w/v, for 3-MeOXAN). This led to concentrations of nanoencapsulated XAN and 3-MeOXAN in the final dispersions of 1173  $\mu\text{g/mL}$  and of 2780  $\mu\text{g/mL}$ , respectively. Thus, the nanocapsule aqueous dispersions developed show higher concentrations for both xanthenes than the respective aqueous solutions as well as the nanosphere dispersions.

Results of particle size analysis (Tables 4 and 5) indicate that the mean sizes of the different nanocapsule formulations are lower than 300 nm and correspond to a mid-range polydispersity population (PI < 0.5). TEM analysis confirmed these results and showed the spherical morphology of XAN and 3-MeOXAN nanocapsules (Fig. 5). Similar particle size results have been previously reported for PLGA nanocapsules containing phenylbutazone [36]. Furthermore, the results show that the mean particle size values of XAN or 3-MeOXAN-loaded nanocapsules do not differ significantly ( $P > 0.05$ ) from those corresponding to empty nanocapsules.

Zeta potential results (Tables 4 and 5) show that both empty and drug-loaded nanocapsules, exhibit a negative charge with values ranging from –41.8 to –36.3 mV. The presence of xanthenes did not affect significantly the zeta potential ( $P > 0.05$ ). Negative zeta potential values of –41 mV have also been previously reported by Marchal-Heussler et al. [37] for PLGA nanocapsules containing

betaxolol. The zeta potential values of the nanocapsules developed in our study may constitute an important contribution for the physical stability of the dispersions. In fact, it is known that high zeta potential values, above 30 mV, either positive or negative, lead to more stable nanocapsule dispersions due to the repulsion between particles, which prevents their aggregation [20]. Our results can be attributed to the specific composition of the nanocapsules (polymer and surfactant concentrations as well as to the type of oil core). According to several authors [20,35,38], the major components of nanocapsules, which can affect their zeta potential are lecithins, oil core, polymer and poloxamer. Lecithins and oils have compounds such as free acids or negatively charged phospholipids, which confer a negative charge to nanocapsules. Polymers, especially poly  $\alpha$ -hydroxy acids, such as poly(DL-lactide), impart negative charge due to carboxyl groups. Poloxamer, a non-ionic surfactant, tends to reduce the absolute value of zeta potential.

### 3.3. In vitro release

The in vitro release profiles of 3-MeOXAN and of XAN from PLGA nanocapsules and from the corresponding control nanoemulsions are shown in Figs. 6 and 7. Nanoemulsions were used as control, in order to investigate the role of polymeric wall on drug release. These figures also show the corresponding release diffusion profiles of the free compounds in aqueous solution through the dialysis bag. The experiments were performed under ‘sink conditions’, in order to avoid the interference of the xanthenes solubility in the in vitro release. As can be observed in both

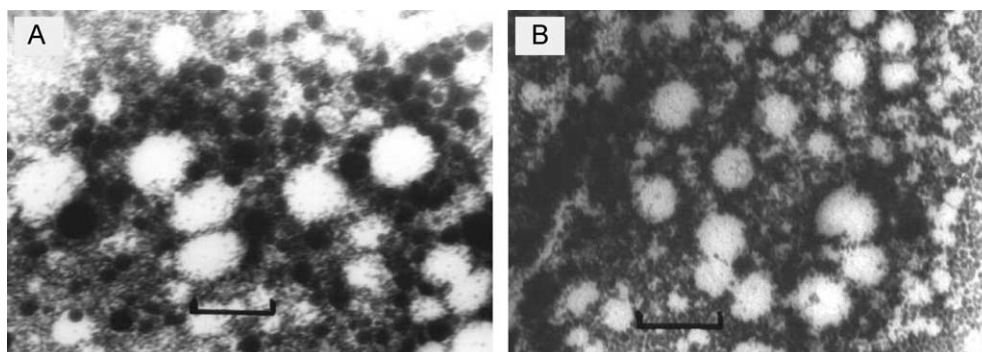


Fig. 5. Transmission electron microphotographs of PLGA nanocapsules containing: (A) XAN or (B) 3-MeOXAN. Scale bar = 250 nm.

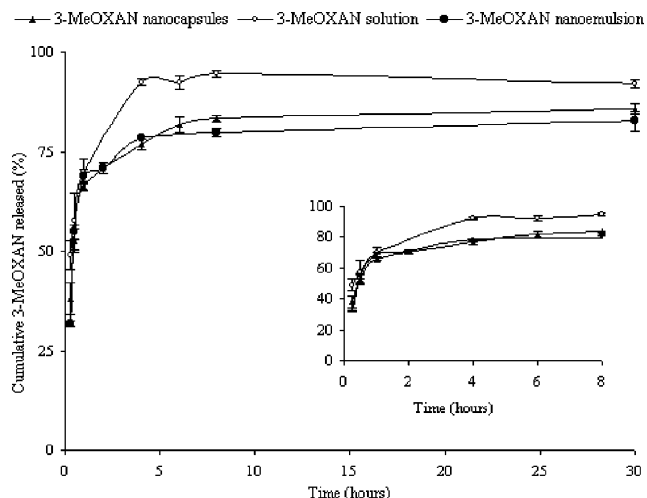


Fig. 6. In vitro release profiles of 3-MeOXAN from PLGA nanocapsules and from nanoemulsion followed by its diffusion through the dialysis bag. The diffusion profile of free 3-MeOXAN dissolved in the medium through the dialysis membrane is shown as a control. The theoretical 3-MeOXAN concentration was, in nanocapsules and nanoemulsion, 3360  $\mu\text{g/mL}$ . Each point represents the mean  $\pm$  SD values obtained from three different batches. The inset shows the release profiles over the first 8 h ( $*P < 0.05$ ).

figures, practically the totality of both xanthenes in solution diffused through the dialysis bag within 4 h. However, when the xanthenes were either nanoencapsulated or incorporated into nanoemulsions, the amounts diffused to the inner side of the dialysis bag were reduced, as was also found by other authors for different substances [33,39].

As can be seen in Fig. 6, the release of 3-MeOXAN from nanocapsules and nanoemulsions yielded similar profiles. In both cases, an important initial release rate of the compound during the first hour and a slower release rate up to the fourth

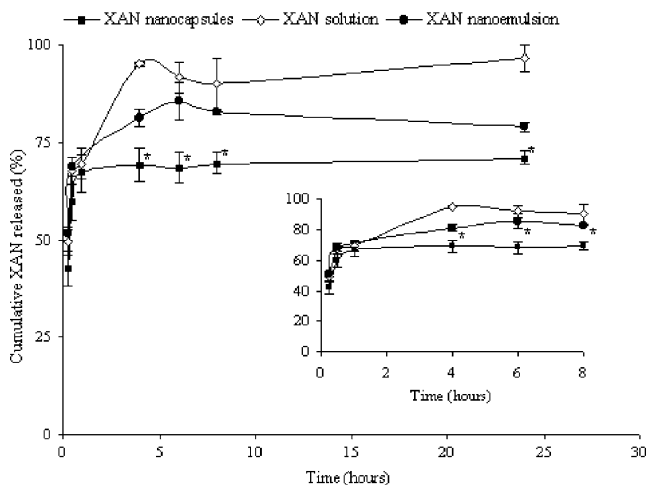


Fig. 7. In vitro release profiles of XAN from PLGA nanocapsules and from nanoemulsion followed by its diffusion through the dialysis bag. The diffusion profile of free XAN dissolved in the medium through the dialysis membrane is shown as a control. The theoretical XAN concentration was, in nanocapsules and nanoemulsion, 1440  $\mu\text{g/mL}$ . Each point represents the mean  $\pm$  SD values obtained from three different batches. The inset shows the release profiles over the first 8 h ( $*P < 0.05$ ).

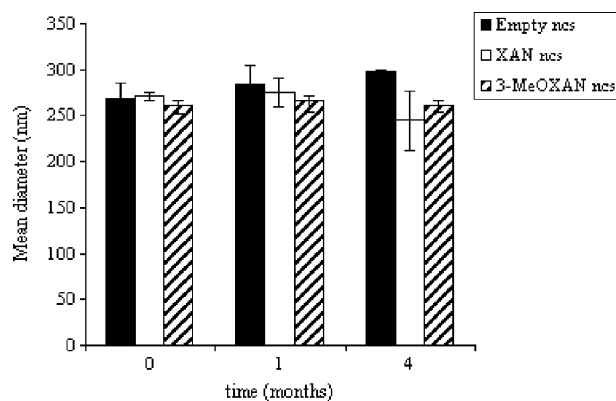


Fig. 8. Evolution of mean size of empty nanocapsules, XAN- and 3-MeOXAN-loaded nanocapsules, during storage at 4  $^{\circ}\text{C}$  for 4 months.

hour were observed. At 1 h of the experiment, the mean amounts of 3-MeOXAN released from nanoemulsion and nanocapsule dispersion were approximately 70% and at 4 h were roughly 80%. Identical release profiles were already reported for other drugs [33,35,36]. The similarity of the release profiles obtained for both systems in the present study evidences that the polymer coating of nanocapsules has no role in the release process of 3-MeOXAN, being the compound's partition between the oily core and the external aqueous medium the main factor governing the process, as was already reported for other drugs [35,36,40].

As can be seen in Fig. 7, the release of XAN from nanocapsules and nanoemulsions yielded different profiles. Despite the important initial release observed for both systems, a significant difference ( $P < 0.05$ ) after the first 30 min and up to the end of the experiment was noted. At 30 min, the mean amounts of XAN released from nanocapsule and nanoemulsion dispersions were  $59.7 \pm 4.3\%$  and  $69.0 \pm 2.5\%$ , respectively. At 4 h. and until the end of the assay, the mean amounts of XAN released from nanocapsule and nanoemulsion dispersions were approximately 70 and 80%, respectively. The different release profiles indicates that another factor besides XAN partition between oil core and the aqueous medium

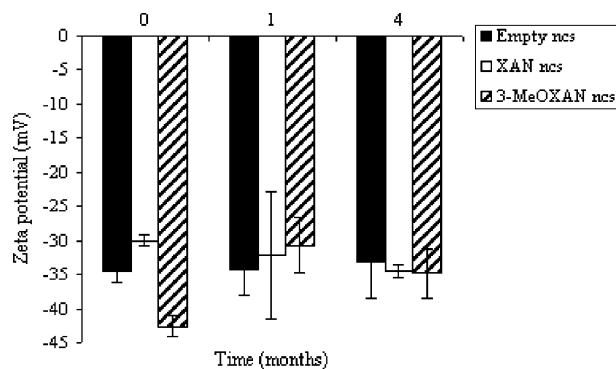


Fig. 9. Evolution of zeta potential of empty nanocapsules, XAN- and 3-MeOXAN-loaded nanocapsules, during storage at 4  $^{\circ}\text{C}$  for 4 months.



influences the release from nanocapsules, which may suggest the existence of an interaction between the compound and the polymer of the nanocapsules. Indeed, as previously reported for other drugs [33], the slower release from the nanocapsules as compared to the emulsion could be attributed to an interaction between the compound and the polymer wall of the nanocapsules.

By comparing the release profiles of both xanthenes from the respective nanoemulsions (Figs. 6 and 7), the aforementioned higher affinity of 3-MeOXAN for *Myrtilol 318* is in accordance with its slower release rate.

The rapid release of different drugs from nanocapsules has been previously reported by different authors [20]. Despite this large burst release, nanocapsules have been shown to improve biological activities of several drugs either in vitro [41] or in vivo when administered by ocular [37] or parenteral [42] routes. Therefore, besides nanocapsule formulations we developed afforded higher concentrations of XAN and 3-MeOXAN than those corresponding to the respective aqueous solutions, these nanocarriers could also be useful for the improvement of biological activity of xanthenes.

### 3.4. Physical stability

Particle size is an important property of colloidal dispersions, since the tendency to sediment is determined by changes in this parameter [43]. Furthermore, particle size influences their in vivo behaviour [44]. As shown in Fig. 8, no significant differences ( $P > 0.05$ ) on the mean size of empty nanocapsules and XAN- or 3-MeOXAN-loaded nanocapsules were observed during storage of the respective aqueous dispersions at 4 °C for 4 months. Similarly, no significant variation on zeta potential values (Fig. 9) was observed during storage for all studied nanocapsule formulations ( $P > 0.05$ ).

Besides the lack of changes in size or zeta potential, the xanthone-loaded nanocapsules remained visually unchanged during storage in the referred conditions. No sediment, cream or free oil could be observed in any formulation. In addition, no XAN crystals were observed for up to 4 months. For 3-MeOXAN-loaded nanocapsules no crystals were detected for up to 3 months. However, some crystals could be observed at the end of the fourth month. Guterres et al. [31] and Schaffazick et al. [45] have also reported the appearance of drug crystals in nanocapsule formulations during storage (after 8 months). According to these authors, this phenomenon could be attributed to the presence of nanocrystals, stabilized by the surfactants, which, with time, start to grow and precipitate.

## 4. Conclusions

The solvent displacement technique adopted in the present work was found to be appropriate for the preparation

of nanoparticle formulations containing either XAN or 3-MeOXAN. This process allowed us to obtain nanospheres of a mean diameter  $< 170$  nm and nanocapsules of a mean diameter  $< 300$  nm. Nanoincorporation of these poorly water-soluble compounds affords the preparation of formulations with higher concentrations of XAN or 3-MeOXAN than those corresponding to the respective aqueous solutions. Nanocapsules appear to be more appropriate carriers for both xanthenes, once encapsulated XAN and 3-MeOXAN concentrations in the final dispersions were 60 and 100-fold, respectively, to those corresponding to nanospheres. 3-MeOXAN release from nanocapsules is governed mainly by its partition between the oil core and the external aqueous medium. The release profile of XAN from nanocapsules suggests the existence of an interaction of the drug with the polymer. Developed nanocapsule formulations were shown to be physically stable for a period of 3–4 months.

## Acknowledgements

This work was supported by Fundação para a Ciência e a Tecnologia (FCT) (Unidade de I & D n°226/94), POCTI (QCA III), FEDER and Praxis XXI. Maribel Teixeira is a recipient of a PhD grant from FCT (Praxis XXI/BD/21841/99).

## References

- [1] V. Peres, T.J. Nagem, F.F. de Oliveira, Tetraoxygenated naturally occurring xanthenes, *Phytochemistry* 55 (2000) 683–710.
- [2] M.M.M. Pinto, E.P. Sousa, Natural and synthetic xanthonolignoids: chemistry and biological activities, *Curr. Med. Chem.* 10 (2003) 1–12.
- [3] C.N. Lin, M.I. Chung, S.J. Liou, T.H. Lee, J.P. Wang, Synthesis and anti-inflammatory effects of xanthone derivatives, *J. Pharm. Pharmacol.* 48 (1996) 532–538.
- [4] E.R. Fernandes, F.D. Carvalho, F.G. Remião, M.L. Bastos, M. Pinto, O.R. Gottlieb, Hepatoprotective activity of xanthenes and xanthonolignoids against *tert*-butylhydroperoxide-induced toxicity in isolated rat hepatocytes comparison with silybin, *Pharm. Res.* 12 (1995) 1756–1760.
- [5] M. Pinto, M.S.J. Nascimento, Anticomplementary activity of hydroxy- and methoxyxanthenes, *Pharm. Pharmacol. Lett.* 7 (1997) 125–127.
- [6] M.J. Gonzalez, M.S.J. Nascimento, H. Cidade, M.M. Pinto, A. Kijjoa, C. Anantachoke, A.M. Silva, W. Herz, Immunomodulatory activity of xanthenes from *Calophyllum teysmannii* var. *inuphyllloide*, *Planta Médica* 65 (1999) 368–371.
- [7] M. Pedro, F. Cerqueira, M.E. Sousa, M.S.J. Nascimento, M. Pinto, Xanthenes as inhibitors of growth of human cancer cell lines and their effects on the proliferation of human lymphocytes in vitro, *Bioorg. Med. Chem.* 10 (2002) 3725–3730.
- [8] L. Saraiva, P. Fresco, E. Pinto, E. Sousa, M. Pinto, J. Gonçalves, Synthesis and in vivo modulatory activity of protein kinase C of xanthone derivatives, *Bioorg. Med. Chem.* 10 (2002) 3219–3277.
- [9] L. Saraiva, P. Fresco, E. Pinto, E. Sousa, M. Pinto, J. Gonçalves, Inhibition of  $\alpha$ ,  $\beta$ I,  $\delta$  and  $\zeta$  protein kinase C isoforms by xanthonolignoids, *J. Enzym. Inhib. Med. Chem.* 18 (2003) 357–370.

- [10] A. Sanches, J.L. Vila-Jato, M.J. Alonso, Development of biodegradable microspheres and nanospheres for the controlled release of cyclosporine A, *Int. J. Pharm.* 99 (1993) 263–273.
- [11] Y.I. Kim, L. Fluckiger, M. Hoffman, I. Lartaud-Idjouadiene, J. Atkinson, P. Maincent, The antihypertensive effect of orally administered nifedipine-loaded nanoparticles in spontaneously hypertensive rats, *Br. J. Pharmacol.* 120 (1997) 399–404.
- [12] C. Fonseca, S. Simões, R. Gaspar, Paclitaxel-loaded PLGA nanoparticles: preparation, physicochemical characterization and in vitro anti-tumoral activity, *J. Control Release* 83 (2002) 273–286.
- [13] M.J. Alonso, Nanoparticulate drug carrier technology in: S. Cohen, H. Bernstein (Eds.), *Microparticulate Systems for the Delivery of Proteins and Vaccines*, Marcel Dekker, New York, 1996, pp. 203–242.
- [14] P. Couvreur, C. Dubernet, F. Puisieux, Controlled drug delivery with nanoparticles: current possibilities and future trends, *Eur. J. Biopharm.* 41 (1995) 2–13.
- [15] P.J. Lowe, C.S. Temple, Calcitonin and insulin in isobutylcyanoacrylate nanocapsules: protection against proteases and effect on intestinal absorption in rats, *J. Pharm. Pharmacol.* 46 (1994) 547–552.
- [16] P. Couvreur, E. Fattal, H. Alphanhary, F. Puisieux, A. Andreumont, Intracellular targeting of antibiotics by means of biodegradable nanoparticles, *J. Control Release* 19 (1992) 259–268.
- [17] R. Jain, N.H. Shah, A.W. Malick, C. Rhodes, Controlled drug delivery by biodegradable poly(ester) devices: different preparative approaches, *Drug Dev. Ind. Pharm.* 24 (1998) 703–727.
- [18] H. Fessi, J.P. Devissaguet, F. Puisieux, C. Thies, Procédé de préparation de systèmes colloïdaux dispersibles d'une substance sous forme de nanoparticules, French Patent, 2,608,988 (1988).
- [19] H. Fessi, F. Puisieux, J.P. Devissaguet, N. Ammoury, S. Benita, Nanocapsule formation by interfacial polymer deposition following solvent displacement, *Int. J. Pharm.* 55 (1989) R1–R4.
- [20] P. Legrand, G. Barratt, V. Mosqueira, H. Fessi, J.P. Devissaguet, Polymeric nanocapsules as drug delivery systems. A review, *STP Pharma Sci.* 9 (1999) 411–418.
- [21] V.C.F. Mosqueira, P. Legrand, H. Pinto-Aphanhary, F. Puisieux, G. Barrat, Poly(D,L-Lactide) nanocapsules prepared by a solvent displacement process: influence of the composition on the physicochemical and structural properties, *J. Pharm. Sci.* 89 (2001) 614–626.
- [22] E.G.R. Fernandes, A.M.S. Silva, J.A.S. Cavaleiro, F.M. Silva, M.F. Borges, M.M.M. Pinto,  $^1\text{H}$  and  $^{13}\text{C}$  spectroscopy of mono-, di-, tri- and tetrasubstituted xanthenes, *Magn. Reson. Chem.* 36 (1998) 305–309.
- [23] M. Teixeira, M.M.M. Pinto, C.M. Barbosa, Validation of a spectrophotometric method for quantification of xanthone in biodegradable nanoparticles, *Pharmazie* 59 (2004) 257–259.
- [24] M. Teixeira, C.M.M. Afonso, M.M.M. Pinto, C.M. Barbosa, A validated HPLC method for assay of xanthone and 3-methoxyxanthone in PLGA nanocapsules, *J. Chromatogr. Sci.* 41 (2003) 371–376.
- [25] M.Y. Levy, S. Benita, Drug release from submicronized O/W emulsion: a new in vitro kinetic evaluation model, *Int. J. Pharm.* 66 (1990) 29–37.
- [26] J.M. Barichello, M. Morishita, K. Takayama, T. Nagai, Encapsulation of hydrophilic and lipophilic drugs in PLGA nanoparticles by the nanoprecipitation method, *Drug Dev. Ind. Pharm.* 25 (1999) 471–476.
- [27] P. Ahlin, J. Kristl, A. Kristl, F. Vrecer, Investigation of polymeric nanoparticles as carriers of enalaprilat for oral administration, *Int. J. Pharm.* 239 (2002) 113–120.
- [28] A.A. Esteller, *Sistemas coloidales*, in: *Fisicoquímica para farmácia y biología*, Ediciones Científicas y Técnicas, Barcelona, Spain, 1992 pp. 925–956.
- [29] M.D. Blanco, M.J. Alonso, Development and characterization of protein-loaded poly(lactide-co-glycolide) nanospheres, *Eur. J. Pharm. Biopharm.* 43 (1997) 287–294.
- [30] T. Govender, S. Stolnik, M.C. Garnett, L. Illum, S. Davis, PLGA nanoparticles prepared by nanoprecipitation: drug loading and release studies of a water soluble drug, *J. Control Release* 57 (1999) 171–185.
- [31] S.S. Guterres, H. Fessi, G. Barratt, J.-P. Devissaguet, F. Puisieux, Poly(DL-lactide) nanocapsules containing diclofenac: I. Formulation and stability study, *Int. J. Pharm.* 113 (1995) 57–63.
- [32] M. Fresta, G. Cavallaro, G. Giammona, E. Wehrli, G. Puglisi, Preparation and characterization of polyethyl-2-cyanoacrylate nanocapsules containing antiepileptic drugs, *Biomaterials* 17 (1996) 751–758.
- [33] V. Ferranti, H. Marchais, C. Chabenat, A.M. Orecchioni, O. Lafont, Primidone-loaded poly-ε-caprolactone nanocapsules: incorporation efficiency and in vitro release profiles, *Int. J. Pharm.* 193 (1999) 107–111.
- [34] P. Calvo, Desarrollo de nuevos sistemas coloidales y su aplicación en la administración tópica y ocular de medicamentos, PhD Thesis, Universidad de Santiago de Compostela, Facultad de Farmacia, Spain (1995) pp.119–160.
- [35] P. Calvo, J.L. Vila Jato, M.J. Alonso, Comparative in vitro evaluation of several colloidal systems, nanoparticles, nanocapsules, and nanoemulsions, as ocular drug carriers, *J. Pharm. Sci.* 85 (1996) 530–536.
- [36] H. Marchais, S. Benali, J. Irache, C. Thrasse-Bloch, O. Lafont, A.M. Orecchioni, Entrapment efficiency and initial release of phenylbutazone from nanocapsules prepared from different polyesters, *Drug Dev. Ind. Pharm.* 24 (1998) 883–888.
- [37] L. Marchal-Heussler, H. Fessi, M. Devissaguet, M. Hoffman, P. Maincent, Colloidal drug delivery systems for the eye. A comparison of the efficacy of three different polymers: polyisobutylcyanoacrylate, polylactic-co-glycolic acid, poly-epsilon-caprolactone, *STP Pharma Sci.* 2 (1992) 98–104.
- [38] C. Losa, L. Marchal-Heussler, F. Orallo, J.L. Vila Jato, M.J. Alonso, Design of new formulations for topical ocular administration: polymeric nanocapsules containing metipranolol, *Pharm. Res.* 10 (1993) 80–87.
- [39] N. Ammoury, H. Fessi, J.P. Devissaguet, F. Puisieux, S. Benita, In vitro release kinetic pattern of indomethacin from poly(D,L-Lactide) nanocapsules, *J. Pharm. Sci.* 79 (1990) 763–767.
- [40] N.S. Santos-Magalhães, A. Pontes, V.M.W. Pereira, M.N.P. Caetano, Colloidal carriers for benzathine penicillin G: nanoemulsions and nanocapsules, *Int. J. Pharm.* 208 (2000) 71–80.
- [41] C. Morin, G. Barrat, H. Fessi, H. J. P. Devissaguet, F. Puisieux, Improved intracellular delivery of muramyl dipeptide analog by means of nanocapsules, *Int. J. Immunopharmacol.* 16 (1994) 451–456.
- [42] G. Barrat, F. Puisieux, W.P. YU, C. Foucher, H. Fessi, J.-P. Devissaguet, Anti-metastatic activity of MDP-L-alanyl-cholesterol incorporated into various types of nanocapsules, *Int. J. Pharm.* 16 (1998) 457–461.
- [43] B. Magenheimer, S. Benita, Nanoparticle Characterization: a comprehensive physicochemical approach, *STP Pharma Sci.* 1 (1991) 221–241.
- [44] R. Bodmeier, P. Maincent, Polymeric dispersions as drug carriers in: H.A. Lieberman, M.M. Rieger, G.S. Banker (Eds.), *Pharmaceutical Dosage Forms: Disperse Systems* vol. 3, Marcel Dekker, New York, 1998, pp. 87–127.
- [45] S. Schaffazick, A. Pohlmann, L. Freitas, S. Guterres, Caracterização e estudo de estabilidade de suspensões de nanocápsulas e de nanoesferas poliméricas contendo diclofenaco, *Acta Farm. Bonaerense* 21 (2002) 99–106.